

Incident direction free wave propagation

L. Jin^{1,*} and Z. Song¹

¹*School of Physics, Nankai University, Tianjin 300071, China*

We propose an incident direction free wave propagation generated by unidirectional destructive interference, which is a consequence of the appropriate match of synthetic magnetic flux and the incident wave vector. Single-direction lasing and one-way propagation are feasible without breaking reciprocity or introducing nonlinearity. Unidirectional destructive interference enables a unidirectional laser and a unidirectional perfect absorber. When they are combined in a parity-time symmetric manner, the spectral singularities vanish with bounded reflection and transmission. Our findings provide insights into light modulation and will shed light on the exploration of desirable asymmetric features of non-Hermitian systems in fundamental research and practical applications.

Parity-time (\mathcal{PT}) symmetry has been extensively investigated in a variety of systems and may enable entirely real spectra in non-Hermitian systems [1–17]. The degree of non-Hermiticity controls the exact and broken \mathcal{PT} -symmetric phases [18–21]. The phase transition point is an exceptional point [22–26], which is utilized for sensitivity enhancement [27–30]; the topology of exceptional points varies in distinct systems [31–35]. Another type of singularity in non-Hermitian systems is the spectral singularity (SS) in a system of infinite size, in which eigenstate completeness is spoiled [36, 37]. The coherent perfect absorber, a time-reversed laser, absorbs incident waves from opposite directions at an appropriate phase match [38–46]. Asymmetric couplings in Hermitian systems can not induce asymmetric scattering, asymmetric scattering is achieved in non-Hermitian systems although the systems are reciprocal [47]. In a \mathcal{PT} -symmetric metamaterial, unidirectional reflectionlessness enables an invisibility cloak at optical frequencies [48]. Unidirectional spectral singularity emerges at the coincidence of independent SS because of the interplay between \mathcal{PT} symmetry and Fano resonance [49]; which enables unidirectional perfect absorption [50] and one-way lasing [51, 52].

In this Letter, we propose an incident direction free wave propagation, which is an extreme asymmetric dynamics that emerges from the special match of synthetic magnetic flux and the incident wave vector. In the proposed system, the reflection and transmission amplitudes switch for the left and right incidences. The dynamics after scattering are identical, independent of the incident direction. This effect stems from unidirectional destructive interference induced by the synthetic magnetic flux. Single-direction lasing occurs at the SS, where the incidence from either side induces a unidirectional lasing in the same direction. With judiciously chosen synthetic magnetic fluxes, detunings, and the gain or loss of side-coupled resonators, the SS exhibits unidirectional lasing or unidirectional perfect absorption. Their coincidence can lead to an SS elimination under \mathcal{PT} symmetry. Moreover, lasing on one side and absorbing on the opposite side is possible. These novel wave propagation phenomena facilitate various applications of non-Hermitian

metamaterials without breaking reciprocity or introducing linearity [52–56].

We consider a one-dimensional uniformly coupled passive resonator chain. All the resonators have an identical resonant frequency ω_c ; the coupling strength is set to be unity ($J = 1$). A resonator is side-coupled to its two nearest resonators in the chain; the system is schematically illustrated in the upper panels of Figs. 1(a) and 1(b). One side-coupling is unity and the other side-coupling is asymmetric, being $e^{\pm i\phi_\alpha}$, and is introduced through the optical path imbalance method, resulting in a synthetic magnetic flux in the closed side-coupled configuration [57]. Figure 1(e) schematically illustrates the coupled resonators. The primary resonators (round-shaped) are evanescently coupled through the auxiliary resonators (stadium-shaped), which are antiresonant with the primary resonators. This structure equivalently induces an effective coupling J between primary resonators [58]. The optical path imbalance induces extra asymmetric phase factors $e^{\pm i2\pi\Delta x/\lambda}$ between the effective primary resonator coupling, and equivalently introduces a synthetic magnetic flux $\phi_\alpha = 2\pi\Delta x/\lambda$, where the path length difference is $2\Delta x$ and λ is the resonant wavelength.

Unidirectional destructive interference.—The synthetic magnetic flux affects interference. At an appropriate synthetic magnetic flux that matches the incident wave vector $\phi_\alpha = \pi \pm k$, the reflectionless transmission occurs for incidences from the left and right directions. In the presence of an asymmetric coupling, transmission and reflection are reciprocal for passive resonators, but the wave functions for opposite incident directions are distinct. The wave function of the system at steady state can be expressed as $f_j = Ae^{ikj} + Be^{-ikj}$ ($j < 0$) and $f_j = Ce^{ikj} + De^{-ikj}$ ($j > 0$) for resonator j . The S -matrix is defined as

$$\begin{pmatrix} B \\ C \end{pmatrix} = S \begin{pmatrix} D \\ A \end{pmatrix}.$$

The wave functions the left and right incidences are $f_j = e^{ikj} + r_L e^{-ikj}$ ($j < 0$), $f_j = t_L e^{ikj}$ ($j > 0$) and $f_j = t_R e^{-ikj}$ ($j < 0$), $f_j = e^{-ikj} + r_R e^{ikj}$ ($j > 0$), respectively.

At $\phi_\alpha = \pi + k$, the side-coupled resonator α is equivalently isolated for the left incidence because of the de-

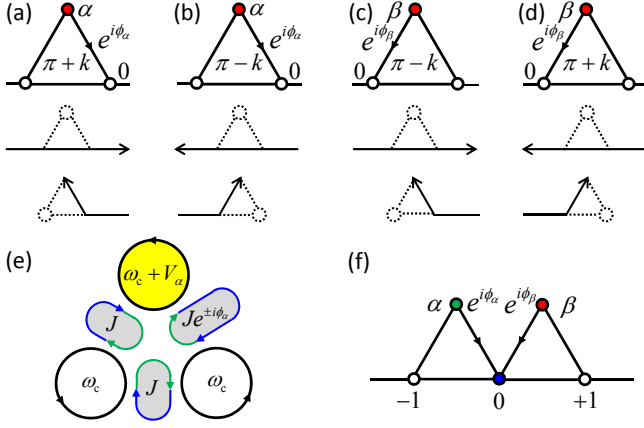


FIG. 1. (a-d) Schematic of the unidirectional perfect absorption. The upper panels illustrate distinct side-coupled configurations with asymmetric coupling; $\phi_{\alpha,\beta}$ values are inside. The central panel illustrates the unidirectional destructive interference from one incident direction and the lower panel illustrates unidirectional perfect absorption from the opposite incident direction, $V_{\alpha,\beta} = -e^{ik}$, and k is the incident wave vector. (e) Schematic of coupled resonators with asymmetric coupling, the blue and green arrows indicate the counterclockwise mode for photons. (f) Schematic of the chain with two side-coupled resonators.

structive interference induced by the synthetic magnetic flux ϕ_α ; the wave function at the side-coupled resonator α is zero. For the right incidence, the wave function of the side-coupled resonator α does not vanish; therefore, the scattering for the right incidence varies according to the detuning Δ_α and loss γ_α of the side-coupled resonator α ($V_\alpha = \Delta_\alpha - i\gamma_\alpha$). The right reflection is still zero, but the right transmission changes into $(e^{ik} + V_\alpha)/(e^{-ik} + V_\alpha)$ [59]. The elements of S -matrix are

$$S = \begin{pmatrix} t_R & r_L \\ r_R & t_L \end{pmatrix} = \begin{pmatrix} (e^{ik} + V_\alpha)/(e^{-ik} + V_\alpha) & 0 \\ 0 & 1 \end{pmatrix}.$$

For a passive resonator α (real V_α), the right incidence is also a resonant transmission, but with a nonvanishing occupation on the side-coupled resonator α .

Unidirectional perfect absorption and unidirectional lasing.—The unidirectional destructive interference provides an opportunity to alter the right scattering without affecting the left scattering and its *reflectionless is bidirectional*; thus, unidirectional destructive interference can enrich unidirectional dynamics. Through introducing a gain or loss, a unidirectional lasing or a unidirectional perfect absorption is realized without breaking reciprocity [49–52]. At $\phi_\alpha = \pi + k$, the left scattering is fixed although V_α varies; the perfect absorption occurs for the right incidence when $V_\alpha = -e^{ik}$ [Fig. 1(a)], where the side-coupled resonator α has a frequency detuning $-\cos k$ and a loss rate $\sin k$. The wave function for the right incidence is $f_j = 0$ ($j < 0$), $f_j = e^{-ikj}$ ($j \geq 0$), and $f_\alpha = -1$, consisting of unidirectional

incoming wave that is completely absorbed at the side-coupled resonator α without reflection [Fig. 1(a)]; $r_L = r_R = t_R = 0$ and $|t_L| = 1$. When the synthetic magnetic flux is opposite $\phi_\alpha = \pi - k$, the wave function is a left-right mirror reflection of the situation of $\phi_\alpha = \pi + k$, in which the side-coupled resonator is isolated for the right incidence [Fig. 1(b)]. Figures 1(c) and 1(d) illustrate the unidirectional perfect absorption for other coupling structures. The unidirectional lasing occurs when $V_\alpha = -e^{-ik}$, where the side-coupled resonator α has an equal amount of gain in contrast to the unidirectional perfect absorption. The wave function for the right incidence is $f_j = e^{-ikj}$ ($j < 0$), $f_j = 0$ ($j \geq 0$), and $f_\alpha = 1$; consisting of a unidirectional outgoing wave that satisfies the boundary condition of lasing without any injection. This unidirectional lasing is a result of right transmission divergence.

Two side-coupled resonators.—The unidirectional destructive interference facilitates the design of optical control devices, leading to the isolation of side-coupled resonators in one incident direction and unidirectional manipulation of the wave propagation. When assembling one more side-coupled resonator, the cooperation between the synthetic magnetic fluxes can result in more intriguing phenomena. Consider a system with two side-coupled resonators as illustrated in Fig. 1(f), in which each side-coupled resonator is coupled to two neighboring resonators in the chain; both side-coupled resonators are coupled to the central resonator 0. The frequency detunings and the non-Hermiticity (gain or loss) of resonators α , β , and 0 are represented by the real and imaginary parts of V_α , V_β , and V_0 , respectively; the non-Hermiticity is modeled by a constant gain or loss rate that is far away from gain saturation [20, 60]. The asymmetric couplings induce synthetic magnetic fluxes, which are associated with the detunings and gain or loss of the side-coupled resonators that control the dynamical process. At appropriate matches, the unidirectional destructive interference, unidirectional perfect absorption, and unidirectional lasing will create novel asymmetric phenomena.

The resonators support the clockwise and counterclockwise modes, they experience opposite synthetic magnetic fluxes. We consider the counterclockwise mode without loss of generality [Fig. 1(e)]. The equations of motion at steady-state yield

$$E_k f_j = -f_{j-1} - f_{j+1}, \quad (1)$$

for resonator $j \neq 0, \pm 1$ on the chain; otherwise,

$$E_k f_{-1} = \omega_c f_{-1} - f_{-2} - f_0 - f_\alpha, \quad (2)$$

$$E_k f_\alpha = (\omega_c + V_\alpha) f_\alpha - f_{-1} - e^{-i\phi_\alpha} f_0, \quad (3)$$

$$E_k f_0 = (\omega_c + V_0) f_0 - f_{-1} - f_1 - e^{i\phi_\alpha} f_\alpha - e^{i\phi_\beta} f_\beta, \quad (4)$$

$$E_k f_\beta = (\omega_c + V_\beta) f_\beta - f_1 - e^{-i\phi_\beta} f_0, \quad (5)$$

$$E_k f_1 = \omega_c f_1 - f_0 - f_2 - f_\beta, \quad (6)$$

where f_j is the wave function of resonator j . The dispersion relation is $E_k = \omega_c - 2 \cos k$.

Incident direction free wave propagation.—The asymmetric couplings significantly affect the interference. We investigate the system at fixed synthetic magnetic fluxes $\phi_\alpha = \phi_\beta = \pi + k$. The side-coupling configuration of resonator β is a left-right mirror reflection of the configuration of resonator α , and the unidirectional destructive interference at resonator β is indicated in Fig. 1(d). Figure 2(a) schematically illustrates the wave propagation for the left incidence; the wave resonantly transmits at resonator α because of the destructive interference caused by the synthetic magnetic flux ϕ_α . Then, the transmitted wave is scattered at resonator 0, and the reflection and transmission coefficients are $r_0 = V_0/(2i \sin k - V_0)$ and $t_0 = r_0 + 1$ [61]. The reflected portion at resonator 0 (cyan arrow) passes through resonator α from the right side without reflection (green arrow) and forms the left reflection; the transmitted portion at resonator 0 (purple arrow) passes through resonator β from the left side without reflection (red arrow) and forms the left transmission. The scattering of resonator 0 is reciprocal; the green (red) arrow represents the reflectionless transmission modulated by resonator α (β). The right reflection and right transmission are similarly obtained [Fig. 2(b)]:

$$r_L = r_0 \frac{e^{ik} + V_\alpha}{e^{-ik} + V_\alpha}, t_L = t_0 \frac{e^{ik} + V_\beta}{e^{-ik} + V_\beta}; \quad (7)$$

$$r_R = r_0 \frac{e^{ik} + V_\beta}{e^{-ik} + V_\beta}, t_R = t_0 \frac{e^{ik} + V_\alpha}{e^{-ik} + V_\alpha}. \quad (8)$$

The synthetic magnetic fluxes allow that the propagating waves in the left (right) chain after scattered are $V_{\beta(\alpha)}$ independent, regardless of the incident direction. This enables an incident direction free wave propagation when $|r_0| = |t_0|$: the left reflection and transmission equal the right transmission and reflection, respectively.

$$|r_L| = |t_R|, |t_L| = |r_R|, \quad (9)$$

which requires $|2 \sin k/V_0| = 1$. The wave impinging from either direction is equally divided at resonator 0 with $|r_0| = |t_0| = \sqrt{1/(2 - 2 \sin \varphi)}$ when $V_0 = 2e^{i\varphi} \sin k$.

The incident direction free wave propagation occurs at

$$\phi_\alpha = \phi_\beta = \pi + k, V_0 = 2e^{i\varphi} \sin k. \quad (10)$$

The amplitudes of the left- and right-going propagating waves after scattering are separately tuned by V_α and V_β , respectively. The wave functions for the left and right incidences are mirror reflection symmetric about resonator 0 when $V_\alpha = V_\beta$; the modulus of $(e^{ik} + V_{\alpha,\beta})/(e^{-ik} + V_{\alpha,\beta})$ is unity for real $V_{\alpha,\beta}$. The system acts as a half-beam splitter in both cases and $|r_L| = |t_R| = |t_L| = |r_R|$.

The resonator β (α) being $V_{\beta(\alpha)} = -e^{ik}$ induces a perfect absorption of the right- (left-) going propagating wave, except when the system is at the SS when

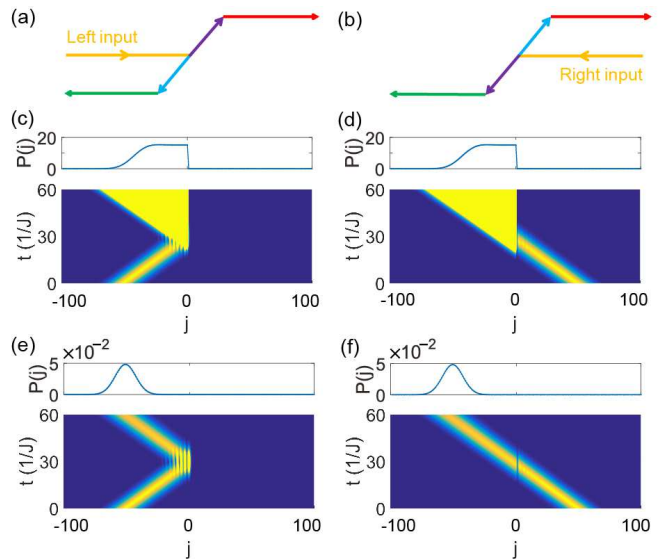


FIG. 2. (a, b) Schematic of the incident direction free wave propagation. (c, d) Simulations of (a, b) single-direction lasing at $V_\alpha = -e^{-ik}$, $V_\beta = -e^{ik}$, and (e, f) one-way propagation at $V_\alpha = -\cos k + 3i \sin k$, $V_\beta = -e^{ik}$. The Gaussian wave packet is $|\Psi(0, j)\rangle = (\sqrt{\pi}/\sigma)^{-1/2} \sum_j e^{-(\sigma^2/2)(j-N_c)^2} e^{ik_c j} |j\rangle$, centered at N_c , where $k_c = \pi/3$ is the wave vector, $\sigma = 0.1$, and j indicates the chain resonator label. The upper panels in (c-f) depict the wave intensities $P(j) = |\Psi(t, j)|^2$ at time $t = 60/J$. Other parameters are $J = 1$, $\phi_\alpha = \phi_\beta = \pi + k$, $V_0 = -2i \sin k$, and $k = \pi/3$.

$V_0 = 2i \sin k$, where outgoing lasing wave is bidirectional; or when $V_{\alpha(\beta)} = -e^{-ik}$, where the outgoing lasing wave is unidirectional toward the left (right) and the propagating wave in the right (left) chain vanishes after scattering. For example, unidirectional lasing occurs when $V_\alpha = -e^{-ik}$, $V_\beta = -e^{ik}$, and $V_0 = -2i \sin k$; the outgoing lasing wave is emitted from the left chain, independent of the incident direction; and the right-going propagating wave vanishes, absorbed at resonator β . The reflection and transmission coefficients are

$$|r_L| = |t_R| \rightarrow \infty, t_L = r_R = 0. \quad (11)$$

The Jost solution of the wave function is $f_j = e^{-ikj}$ ($j < 0$), $f_j = 0$ ($j \geq 0$), $f_\alpha = 1$, and $f_\beta = 0$; consisting of the outgoing wave in the left chain. For an incidence from either direction, the lasing wave is emitted in a single direction: leftward. The simulation of the lasing wave emission is depicted in Figs. 2(c) and 2(d). A Gaussian wave packet excites the wave emission, characterized by a Gaussian error function and its intensity increases linearly [62]. At $V_0 = 2i \sin k$, lasing is bidirectional when $V_{\alpha,\beta} \neq -e^{ik}$; the wave emission is symmetric when $V_{\alpha,\beta}$ is real, but asymmetric when complex $V_\alpha \neq V_\beta$; for $V_{\alpha(\beta)} = -e^{ik}$, the wave emission is absorbed at resonator α (β) and the lasing becomes unidirectional with vanishing emission toward the left (right).

For $V_\alpha = V_\beta = -e^{-ik}$, lasing is bidirectional and V_0 controls the asymmetry of the lasing amplitude.

Another intriguing phenomenon is one-way propagation: the wave is completely reflected without transmission for the left incidence, but completely transmitted without reflection for the right incidence [Figs. 2(e) and 2(f)]. This occurs at $V_\alpha = -\cos k + 3^{\pm 1}i \sin k$, $V_\beta = -e^{ik}$, and $V_0 = -2i \sin k$. Resonator β unidirectionally absorbs the right-going propagating wave. Resonator α tunes the amplitude of the left-going propagating wave. The system rectifies the wave with $|r_L| = |t_R| = 1$ and $t_L = r_R = 0$, previously designed in a nonlinear system with an asymmetric structure [54].

For $V_0 = 0$, the scattering is incident direction dependent. The left and right reflections are both zero when $V_{\alpha,\beta} \neq -e^{-ik}$. The left (right) transmission depends on $V_{\beta(\alpha)}$; the complex $V_{\alpha,\beta}$ with gain (loss) that induces amplification (attenuation). When $V_\alpha = V_\beta = -e^{-ik}$, the transmission diverges with finite reflection. When $V_\alpha = V_\beta = -e^{ik}$, the system acts as a perfect absorber, completely absorbing the incidence from either direction without reflection. When $V_\alpha = -e^{-ik}$ and $V_\beta = -e^{ik}$, unidirectional lasing occurs with $|r_L| = 1$, $t_L = r_R = 0$, and $|t_R| \rightarrow \infty$ (square in Fig. 3).

\mathcal{PT} -symmetric side-coupled resonators.—The Hamiltonians of the unidirectional perfect absorber and the unidirectional laser form a Hermitian conjugation pair. Their SS coincide and vanish at series connection of the two structures in a \mathcal{PT} -symmetric manner. The emission is absorbed and leaves finite scattering intensities [59].

Figure 3 depicts the reflections and transmissions as functions of synthetic magnetic fluxes for $V_\alpha = -e^{-ik}$ and $V_\beta = -e^{ik}$. $|\phi_{\alpha(\beta)}| = 2\pi/3$ produces a wave emission (absorption). $|r_L| = 1$ at $|\phi_\beta| = 2\pi/3$ and $|r_L| \rightarrow \infty$ at $|\phi_\alpha| = 2\pi/3$ and $|\phi_\beta| \neq 2\pi/3$ [Fig. 3(a)]. $V_\beta = -e^{ik}$ results in $f_0 = 0$ for the right incidence except when r_L diverges; consequently, $r_R = 0$. t_L and t_R are depicted in Figs. 3(b) and 3(c). They satisfy $t_L(\phi_\alpha, \phi_\beta) = t_R(-\phi_\alpha, -\phi_\beta)$. t_L diverges at $\phi_\alpha = 2\pi/3$, vanishes at $\phi_\beta = -2\pi/3$, and becomes unity at $\phi_\alpha = 2\pi/3$ and $\phi_\beta = -2\pi/3$, where the SS of the side-coupled structures α and β coincide. Figure 3(d) illustrates the scattering coefficients at $|\phi_\alpha| = 2\pi/3$ (r_L divergence), which are implied by the dash-dotted blue line [t_L in Fig. 3(b)] and solid red line [t_R in Fig. 3(c)]. At $\phi_\alpha + \phi_\beta = 0$, the system is \mathcal{PT} -symmetric; the scattering coefficients converge and lasing vanishes when $\phi_\alpha = -\phi_\beta = \pm 2\pi/3$ [59]. The \mathcal{PT} symmetry ensures that the persistent emission from resonator α is directly absorbed at resonator β to form a unity transmission. The scattering amplitudes are $|r_L| = |t_L| = |t_R| = 1$ and $|r_R| = 0$, and the SS vanishes. At $\phi_\alpha = \phi_\beta = 2\pi/3$, a persistent right-going wave emission for the left incidence and a perfect absorption for the right incidence occur: $|r_L| = 1$, $|t_L| \rightarrow \infty$, and $r_R = t_R = 0$ (circle in Fig. 3). At $\phi_\alpha = \phi_\beta = -2\pi/3$, a persistent left-going wave emission for the right incidence

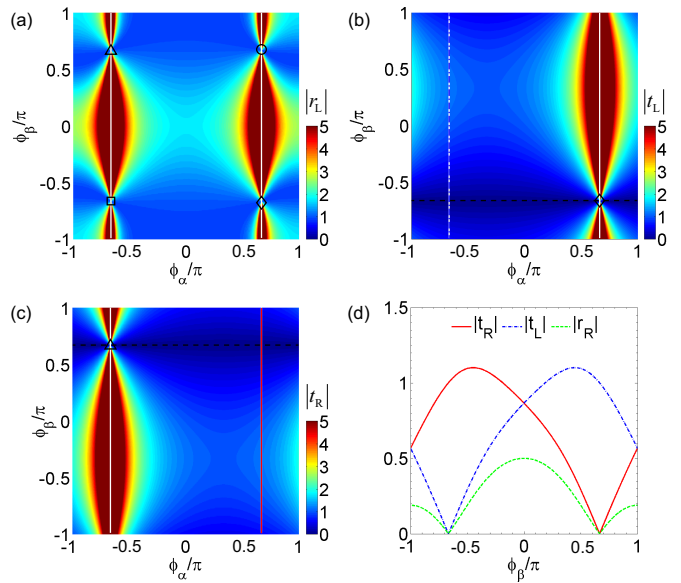


FIG. 3. Contour plots of (a) r_L , (b) t_L , and (c) t_R as functions of ϕ_α and ϕ_β . $r_R = 0$ for $|\phi_\alpha| \neq 2\pi/3$. (d) t_L (t_R) for $\phi_\alpha = -2\pi/3$ ($2\pi/3$) and r_R at when r_L diverges. The solid white lines indicate the divergence and the dashed black lines indicate zero at the SS. Two SS coincide at the marked points, where the values are unity. The reflection and transmission amplitudes are cut to 5. The system parameters are $V_\alpha = -e^{-ik}$, $V_\beta = -e^{ik}$, $V_0 = 0$, and $k = \pi/3$.

and a perfect reflection for the left incidence occur.

Conclusion and discussion.—In summary, we have proposed an incident direction free wave propagation generated by unidirectional destructive interference. The dynamics after scattering are identical for incidences impinging from the left and right directions, which is a consequence of the match of synthetic magnetic flux and the incident wave vector. The interference provides an elite interpretation for the scattering behavior in the side-coupled structure. At the SS, the incident direction free scattering leads to a unidirectional lasing toward single definite direction; additionally, one-way propagation is demonstrated. The \mathcal{PT} symmetry eliminates the SS of the unidirectional lasing and the unidirectional perfect absorption when they coincide where the scattering coefficients are bounded.

The influences of side-coupled resonators vary according to different matches of the synthetic magnetic fluxes. If we set system parameters at when single-direction lasing, but with the opposite synthetic magnetic fluxes, the scattering for the left (right) incidence is resonator β (α) independent and an incidence from one direction induces bidirectional lasing, but an incidence from the opposite direction induces perfect absorption [59]. The lasing amplitudes toward the left and the right are tuned by resonator 0 and reduced to unidirectional when $V_0 = 0$.

A unidirectional perfect absorber prevents a backward flow without affecting the forward propagation, which is a

versatile building block for light control and modulation. By connecting a configuration with left full transmission and right full absorption on the left side of the scattering center in the situation marked by the circle in Fig. 3(a), we obtain a reflectionless unidirectional lasing toward the right for a left incidence and perfect absorption for a right incidence. Moreover, transmissionless unidirectional lasing and perfect absorption is feasible [59]. Our findings open up new directions in designing the novel lasers and optical control devices including but not limited to laser, absorber, rectifier, isolator, and modulator in a variety of areas in optics and beyond.

This work was supported by NSFC (Grant No. 11605094) and the Tianjin Natural Science Foundation (Grant No. 16JCYBJC40800).

* jinliang@nankai.edu.cn

- [1] C. M. Bender, S. Boettcher, *Phys. Rev. Lett.* **80**, 5243 (1998).
- [2] A. Mostafazadeh, *J. Math. Phys.* **43**, 205 (2002).
- [3] H. F. Jones, *J. Phys. A* **38**, 1741 (2005).
- [4] A. Ruschhaupt, F. Delgado, and J. G. Muga, *J. Phys. A* **38**, L171 (2005).
- [5] R. El-Ganainy, K. G. Makris, D. N. Christodoulides, and Z. H. Musslimani, *Opt. Lett.* **32**, 2632 (2007).
- [6] Z. H. Musslimani, K. G. Makris, R. El-Ganainy, and D. N. Christodoulides, *Phys. Rev. Lett.* **100**, 030402 (2008).
- [7] S. Klaiman, U. Günther, and N. Moiseyev, *Phys. Rev. Lett.* **101**, 080402 (2008).
- [8] L. Jin and Z. Song, *Phys. Rev. A* **80**, 052107 (2009).
- [9] Z. Lin, H. Ramezani, T. Eichelkraut, T. Kottos, H. Cao, and D. N. Christodoulides, *Phys. Rev. Lett.* **106**, 213901 (2011).
- [10] M. Liertzer, L. Ge, A. Cerjan, A. D. Stone, H. E. Türeci, and S. Rotter, *Phys. Rev. Lett.* **108**, 173901 (2012).
- [11] D. A. Zezyulin and V. V. Konotop, *Phys. Rev. Lett.* **108**, 213906 (2012).
- [12] H. Jing, S. K. Özdemir, X.-Y. Lü, J. Zhang, L. Yang, and F. Nori, *Phys. Rev. Lett.* **113**, 053604 (2014).
- [13] L. Ge and A. D. Stone, *Phys. Rev. X* **4**, 031011 (2014).
- [14] X. Zhu, H. Ramezani, C. Shi, J. Zhu, and X. Zhang, *Phys. Rev. X* **4**, 031042 (2014).
- [15] L. Chang, X. Jiang, S. Hua, C. Yang, J. Wen, L. Jiang, G. Li, G. Wang, and M. Xiao, *Nat. Photonics* **8**, 524 (2014).
- [16] R. Fleury, D. Sounas, and A. Alù, *Nat. Commun.* **6**, 5905 (2015).
- [17] S. V. Suchkov, F. Fotsa-Ngaffo, A. Kenfack-Jiotsa, A. D. Tikeng, T. C. Kofane, Y. S. Kivshar, and A. A. Sukhorukov, *New J. Phys.* **18**, 065005 (2016).
- [18] A. Guo, G. J. Salamo, D. Duchesne, R. Morandotti, M. Volatier-Ravat, V. Aimez, G. A. Siviloglou, and D. N. Christodoulides, *Phys. Rev. Lett.* **103**, 093902 (2009).
- [19] C. E. Rüter, K. G. Makris, R. El-Ganainy, D. N. Christodoulides, M. Segev, and D. Kip, *Nat. Phys.* **6**, 192 (2010).
- [20] B. Peng, S. K. Özdemir, F. Lei, F. Monifi, M. Gianfreda, G. L. Long, S. Fan, F. Nori, C. M. Bender, and L. Yang, *Nat. Phys.* **10**, 394 (2014).
- [21] Z. Zhang, Y. Zhang, J. Sheng, L. Yang, M.-A. Miri, D. N. Christodoulides, B. He, Y. Zhang, and M. Xiao, *Phys. Rev. Lett.* **117**, 123601 (2016).
- [22] C. Dembowski, B. Dietz, H.-D. Gräf, H. L. Harney, A. Heine, W. D. Heiss, and A. Richter, *Phys. Rev. E* **69**, 056216 (2004).
- [23] H. Cartarius, J. Main, and G. Wunner, *Phys. Rev. Lett.* **99**, 173003 (2007).
- [24] M. Müller and I. Rotter, *J. Phys. A: Math. Theor.* **41**, 244018 (2008).
- [25] R. Uzdin, A. Mailybaev, and N. Moiseyev, *J. Phys. A* **44**, 435302 (2011).
- [26] W. D. Heiss, *J. Phys. A: Math. Theor.* **45**, 444016 (2012).
- [27] J. Wiersig, *Phys. Rev. Lett.* **112**, 203901 (2014).
- [28] Z.-P. Liu, J. Zhang, S. K. Özdemir, B. Peng, H. Jing, X.-Y. Lü, C.-W. Li, L. Yang, F. Nori, and Y. Liu, *Phys. Rev. Lett.* **117**, 110802 (2016).
- [29] W. Chen, S. K. Özdemir, G. Zhao, J. Wiersig, and L. Yang, *Nature (London)* **548**, 192 (2017).
- [30] H. Hodaiei, A. U. Hassan, S. Wittek, H. Garcia-Gracia, R. El-Ganainy, D. N. Christodoulides, and M. Khajavikhan, *Nature (London)* **548**, 187 (2017).
- [31] B. Zhen, C. W. Hsu, Y. Igarashi, L. Lu, I. Kaminer, A. Pick, S.-L. Chua, J. D. Joannopoulos, and M. Soljačić, *Nature (London)* **525**, 354 (2015).
- [32] H. Menke, M. Klett, H. Cartarius, J. Main, and G. Wunner, *Phys. Rev. A* **93**, 013401 (2016).
- [33] J. Doppler, A. A. Mailybaev, J. Böhm, U. Kuhl, A. Girschik, F. Libisch, T. J. Milburn, P. Rabl, N. Moiseyev, and S. Rotter, *Nature (London)* **537**, 76 (2016).
- [34] H. Xu, D. Mason, L. Jiang, and J. G. E. Harris, *Nature (London)* **537**, 80 (2016).
- [35] K. Ding, G. Ma, M. Xiao, Z. Q. Zhang, and C. T. Chan, *Phys. Rev. X* **6**, 021007 (2016).
- [36] A. Mostafazadeh, *Phys. Rev. Lett.* **102**, 220402 (2009).
- [37] A. Mostafazadeh, *Phys. Rev. Lett.* **110**, 260402 (2013).
- [38] Y. D. Chong, L. Ge, H. Cao, and A. D. Stone, *Phys. Rev. Lett.* **105**, 053901 (2010).
- [39] S. Longhi, *Phys. Rev. A* **82**, 031801(R) (2010).
- [40] Y. D. Chong, L. Ge, and A. D. Stone, *Phys. Rev. Lett.* **106**, 093902 (2011).
- [41] W. Wan, Y. Chong, L. Ge, H. Noh, A. D. Stone, and H. Cao, *Science* **331**, 889 (2011).
- [42] Y. Sun, W. Tan, H. Li, J. Li, and H. Chen, *Phys. Rev. Lett.* **112**, 143903 (2014).
- [43] Z. J. Wong, Y.-L. Xu, J. Kim, K. O'Brien, Y. Wang, L. Feng, and X. Zhang, *Nat. Photon.* **10**, 796 (2016).
- [44] C. Hang, G. Huang, and V. V. Konotop, *New. J. Phys.* **18**, 085003 (2016).
- [45] L. Ge and L. Feng, *Phys. Rev. A* **95**, 013813 (2017).
- [46] D. G. Baranov, A. Krasnok, T. Shegai, A. Alù, and Y. Chong, *Nat. Rev. Mater.* **2**, 17064 (2017).
- [47] L. Jin, X. Z. Zhang, G. Zhang, and Z. Song, *Sci. Rep.* **6**, 20976 (2016).
- [48] L. Feng, Y.-L. Xu, W. S. Fegadolli, M.-H. Lu, J. E. B. Oliveira, V. R. Almeida, Y.-F. Chen, and A. Scherer, *Nat. Mater.* **12**, 108 (2013).
- [49] H. Ramezani, H.-K. Li, Y. Wang, and X. Zhang, *Phys. Rev. Lett.* **113**, 263905 (2014).
- [50] H. Ramezani, Y. Wang, E. Yablonovitch, and X. Zhang, *IEEE J. Sel. Top. Quantum Electron.* **22**, 115 (2016).
- [51] B. Peng, S. K. Özdemir, M. Liertzer, W. Chen, J.

- Kramer, H. Yilmaz, J. Wiersig, S. Rotter, and Lan Yang, Proc. Natl. Acad. Sci. USA **113**, 6845 (2016).
- [52] H. Ramezani, S. Kalish, I. Vitebskiy, and T. Kottos, Phys. Rev. Lett. **112**, 043904 (2014).
- [53] S. Longhi, D. Gatti, and G. Della Valle, Phys. Rev. B **92**, 094204 (2015).
- [54] S. Lepri and G. Casati, Phys. Rev. Lett. **106**, 164101 (2011).
- [55] J. D'Ambroise, P. G. Kevrekidis, and S. Lepri, J. Phys. A: Math. Theor. **45**, 444012 (2012).
- [56] V. V. Konotop, J. Yang, and D. A. Zezyulin, Rev. Mod. Phys. **88**, 035002 (2016).
- [57] M. Hafezi, Phys. Rev. Lett. **112**, 210405 (2014).
- [58] M. Hafezi, Int. J. Mod. Phys. B **28**, 1441002 (2014).
- [59] See Supplemental Material for the details on derivation of scattering coefficients and simulations of dynamics.
- [60] L. Feng, Z. J. Wong, R.-M. Ma, Y. Wang, and X. Zhang, Science **346**, 972 (2014).
- [61] W. Kim, L. Covaci, and F. Marsiglio, Phys. Rev. B **74**, 205120 (2006).
- [62] P. Wang, L. Jin, G. Zhang, and Z. Song, Phys. Rev. A **94**, 053834 (2016).

SUPPLEMENTARY MATERIAL

A: Scattering coefficients of one side-coupled resonator

We consider a resonator α side-coupled to a uniform chain. The wave functions at steady state are $f_j = Ae^{-ikj} + Be^{ikj}$ ($j < 0$) and $f_j = Ce^{-ikj} + De^{ikj}$ ($j > 0$) for site j . The equations of motion at steady state are reduced to

$$(-e^{-ik} - e^{ik})(Ae^{-ik} + Be^{ik}) = -(Ae^{-2ik} + Be^{2ik}) - f_0 - f_\alpha, \quad (12)$$

$$(-e^{-ik} - e^{ik} - V_\alpha)f_\alpha = -(Ae^{-ik} + Be^{ik}) - e^{-i\phi_\alpha}f_0, \quad (13)$$

$$(-e^{-ik} - e^{ik})f_0 = -(Ae^{-ik} + Be^{ik}) - (Ce^{ik} + De^{-ik}) - e^{i\phi_\alpha}f_\alpha, \quad (14)$$

$$(-e^{-ik} - e^{ik})(Ce^{ik} + De^{-ik}) = -f_0 - (Ce^{2ik} + De^{-2ik}), \quad (15)$$

simplify the equations above, the coefficients satisfy

$$(-e^{ik} - V_\alpha)A + (-e^{-ik} - V_\alpha)B - (-e^{-i\phi_\alpha} - e^{-ik} - e^{ik} - V_\alpha)(C + D) = 0, \quad (16)$$

$$(Ae^{-ik} + Be^{ik}) + e^{i\phi_\alpha}(A + B - C - D) - e^{-ik}C - e^{ik}D = 0. \quad (17)$$

When $\phi_\alpha = \pi + k$, we have $B = 0$, $C = 1$ for $A = 1$, $D = 0$; and $C = 0$, $B = (e^{ik} + V_\alpha)/(e^{-ik} + V_\alpha)$ for $A = 0$, $D = 1$. Therefore, $r_L = r_R = 0$, $t_L = 1$, and $t_R = (e^{ik} + V_\alpha)/(e^{-ik} + V_\alpha)$. The S -matrix is

$$S = \begin{pmatrix} \frac{e^{ik} + V_\alpha}{e^{-ik} + V_\alpha} & 0 \\ 0 & 1 \end{pmatrix}. \quad (18)$$

When $\phi_\alpha = \pi - k$, we have $B = 0$, $C = (e^{ik} + V_\alpha)/(e^{-ik} + V_\alpha)$ for $A = 1$, $D = 0$; and $C = 0$, $B = 1$ for $A = 0$, $D = 1$. Therefore, $r_L = r_R = 0$, $t_L = (e^{ik} + V_\alpha)/(e^{-ik} + V_\alpha)$, and $t_R = 1$. The S -matrix is

$$S = \begin{pmatrix} 1 & 0 \\ 0 & \frac{e^{ik} + V_\alpha}{e^{-ik} + V_\alpha} \end{pmatrix}. \quad (19)$$

B: Scattering coefficients of two side-coupled resonators

Substituting the steady state wave functions into the equations of motion at steady state, we have

$$(-e^{-ik} - e^{ik})(Ae^{-ik} + Be^{ik}) = -(Ae^{-2ik} + Be^{2ik}) - f_0 - f_\alpha, \quad (20)$$

$$(-e^{-ik} - e^{ik} - V_\alpha)f_\alpha = -(Ae^{-ik} + Be^{ik}) - e^{-i\phi_\alpha}f_0, \quad (21)$$

$$(-e^{-ik} - e^{ik} - V_0)f_0 = -(Ae^{-ik} + Be^{ik}) - (Ce^{ik} + De^{-ik}) - e^{i\phi_\alpha}f_\alpha - e^{i\phi_\beta}f_\beta, \quad (22)$$

$$(-e^{-ik} - e^{ik} - V_\beta)f_\beta = -(Ce^{ik} + De^{-ik}) - e^{-i\phi_\beta}f_0, \quad (23)$$

$$(-e^{-ik} - e^{ik})(Ce^{ik} + De^{-ik}) = -f_0 - (Ce^{2ik} + De^{-2ik}) - f_\beta, \quad (24)$$

simplified the equations, we have

$$f_\alpha = A + B - f_0, \quad (25)$$

$$(e^{ik} + V_\alpha)A + (e^{-ik} + V_\alpha)B = (e^{-ik} + e^{ik} + V_\alpha + e^{-i\phi_\alpha})f_0, \quad (26)$$

$$(e^{-ik} + e^{i\phi_\alpha})A + (e^{ik} + e^{i\phi_\alpha})B + (e^{ik} + e^{i\phi_\beta})C + (e^{-ik} + e^{i\phi_\beta})D = (e^{-ik} + e^{ik} + V_0 + e^{i\phi_\alpha} + e^{i\phi_\beta})f_0, \quad (27)$$

$$(e^{-ik} + V_\beta)C + (e^{ik} + V_\beta)D = (e^{-ik} + e^{ik} + V_\beta + e^{-i\phi_\beta})f_0, \quad (28)$$

$$f_\beta = C + D - f_0. \quad (29)$$

For left incidence $D = 0$, we obtain the left reflection $r_L = B/A$ and left transmission $t_L = C/A$,

$$r_L = \frac{(e^{ik} + V_\alpha)[(e^{i\phi_\alpha} + e^{-ik} + V_0)(e^{-ik} + V_\beta) - (e^{ik} + e^{-i\phi_\beta})(e^{i\phi_\beta} + e^{ik})] - (e^{-ik} + e^{ik} + V_\alpha + e^{-i\phi_\alpha})(e^{-ik} + V_\beta)(e^{i\phi_\alpha} + e^{-ik})}{(e^{-ik} + V_\alpha)[(e^{ik} + e^{-i\phi_\beta})(e^{i\phi_\beta} + e^{ik}) - (e^{i\phi_\alpha} + e^{-ik} + V_0)(e^{-ik} + V_\beta)] + (e^{-ik} + e^{ik} + V_\alpha + e^{-i\phi_\alpha})(e^{-ik} + V_\beta)(e^{i\phi_\alpha} + e^{ik})}, \quad (30)$$

$$t_L = \frac{(e^{-ik} + V_\beta + e^{ik} + e^{-i\phi_\beta})[(e^{ik} + V_\alpha)(e^{i\phi_\alpha} + e^{ik}) - (e^{-ik} + V_\alpha)(e^{i\phi_\alpha} + e^{-ik})]}{(e^{-ik} + V_\alpha)[(e^{ik} + e^{-i\phi_\beta})(e^{i\phi_\beta} + e^{ik}) - (e^{-ik} + V_0 + e^{i\phi_\alpha})(e^{-ik} + V_\beta)] + (e^{-ik} + e^{ik} + V_\alpha + e^{-i\phi_\alpha})(e^{-ik} + V_\beta)(e^{i\phi_\alpha} + e^{ik})},$$

For right incidence of $A = 0$, we obtain the right transmission $t_R = B/D$ and right reflection $r_R = C/D$,

$$r_R = \frac{(e^{ik} + V_\beta)[(e^{i\phi_\beta} + e^{-ik} + V_0)(e^{-ik} + V_\alpha) - (e^{ik} + e^{-i\phi_\alpha})(e^{ik} + e^{i\phi_\alpha})] - (e^{-ik} + e^{ik} + V_\beta + e^{-i\phi_\beta})(e^{-ik} + V_\alpha)(e^{-ik} + e^{i\phi_\beta})}{(e^{-ik} + V_\beta)[(e^{ik} + e^{-i\phi_\alpha})(e^{ik} + e^{i\phi_\alpha}) - (e^{-ik} + V_\alpha)(e^{i\phi_\beta} + e^{-ik} + V_0)] + (e^{-ik} + e^{ik} + V_\beta + e^{-i\phi_\beta})(e^{-ik} + V_\alpha)(e^{ik} + e^{i\phi_\beta})}, \quad (31)$$

$$t_R = \frac{(e^{-ik} + e^{ik} + V_\alpha + e^{-i\phi_\alpha})[(e^{ik} + e^{i\phi_\beta})(e^{ik} + V_\beta) - (e^{-ik} + e^{i\phi_\beta})(e^{-ik} + V_\beta)]}{(e^{-ik} + V_\beta)[(e^{ik} + e^{i\phi_\alpha})(e^{ik} + e^{-i\phi_\alpha}) - (e^{-ik} + V_\alpha)(e^{i\phi_\beta} + e^{-ik} + V_0)] + (e^{-ik} + e^{ik} + V_\beta + e^{-i\phi_\beta})(e^{-ik} + V_\alpha)(e^{ik} + e^{i\phi_\beta})}.$$

The interference is elite when the system is not at spectral singularities. In case of $e^{ik} + e^{-i\phi_\beta} = 0$, r_L and t_L are irrelevant to V_β , the side-coupled resonator β is isolated ($f_\beta = 0$) due to the destructive interference for left incidence; thus, the scattering is only affected by V_α and V_0 . On the contrary, when $e^{ik} + e^{-i\phi_\alpha} = 0$, resonator α is isolated and r_R and t_R are irrelevant to V_α . When $e^{ik} + e^{i\phi_\beta} = 0$, r_L and t_R are V_β irrelevant. This indicates that V_β does not affect the left-going waves (for both sides incidence). Similarly, when $e^{ik} + e^{i\phi_\alpha} = 0$, t_L and r_R are V_α irrelevant; V_α does not affect the right-going waves (for both sides incidence).

In the combination of $e^{ik} + e^{i\phi_\alpha} = 0$ and $e^{ik} + e^{i\phi_\beta} = 0$, e.g., $\phi_\alpha = \pi + k$, $\phi_\beta = \pi + k$. The left reflection and right transmission coefficients (the left-going waves) are V_β irrelevant; the left transmission and right reflection coefficients (the right-going waves) are V_α irrelevant. The reflections and transmissions reduce to

$$r_L = \frac{-(e^{ik} + V_\alpha) V_0}{(e^{-ik} + V_\alpha)(e^{i\phi_\alpha} + e^{-ik} + V_0)}, t_L = \frac{(e^{ik} + V_\beta)(e^{i\phi_\alpha} + e^{-ik})}{(e^{-ik} + V_0 + e^{i\phi_\alpha})(e^{-ik} + V_\beta)}, \quad (32)$$

$$r_R = \frac{-(e^{ik} + V_\beta) V_0}{(e^{-ik} + V_\beta)(e^{i\phi_\beta} + e^{-ik} + V_0)}, t_R = \frac{(e^{ik} + V_\alpha)(e^{-ik} + e^{i\phi_\beta})}{(e^{-ik} + V_\alpha)(e^{i\phi_\beta} + e^{-ik} + V_0)}. \quad (33)$$

In the combination of $e^{ik} + e^{-i\phi_\alpha} = 0$ and $e^{ik} + e^{-i\phi_\beta} = 0$, e.g., $\phi_\alpha = \pi - k$, $\phi_\beta = \pi - k$. The left (right) transmission and reflection coefficients are $V_{\beta(\alpha)}$ irrelevant. The reflections and transmissions reduce to

$$r_L = \frac{(e^{ik} + V_\alpha) V_0}{(e^{-ik} + V_\alpha)(e^{i\phi_\alpha} + e^{ik} - V_0)}, t_L = \frac{(e^{ik} + V_\alpha)(e^{i\phi_\alpha} + e^{ik})}{(e^{-ik} + V_\alpha)(e^{i\phi_\alpha} + e^{ik} - V_0)}, \quad (34)$$

$$r_R = \frac{(e^{ik} + V_\beta) V_0}{(e^{-ik} + V_\beta)(e^{ik} + e^{i\phi_\beta} - V_0)}, t_R = \frac{(e^{ik} + V_\beta)(e^{ik} + e^{i\phi_\beta})}{(e^{-ik} + V_\beta)(e^{ik} + e^{i\phi_\beta} - V_0)}. \quad (35)$$

In the combination of $e^{ik} + e^{i\phi_\alpha} = 0$ and $e^{ik} + e^{-i\phi_\beta} = 0$, e.g., $\phi_\alpha = \pi + k$, $\phi_\beta = \pi - k$. The left transmission is the side-coupled resonators α and β irrelevant; the left reflection is resonator β irrelevant. The reflections and transmissions reduce to

$$r_L = -\frac{(e^{ik} + V_\alpha) V_0}{(e^{-ik} + V_\alpha)(e^{i\phi_\alpha} + e^{-ik} + V_0)}, t_L = \frac{e^{i\phi_\alpha} + e^{-ik}}{e^{-ik} + V_0 + e^{i\phi_\alpha}}, \quad (36)$$

$$r_R = \frac{(e^{ik} + V_\beta) V_0}{(e^{-ik} + V_\beta)(e^{ik} + e^{i\phi_\beta} - V_0)}, t_R = \frac{(e^{ik} + V_\beta)(e^{ik} + V_\alpha)(e^{ik} + e^{i\phi_\beta})}{(e^{-ik} + V_\beta)(e^{-ik} + V_\alpha)(e^{ik} + e^{i\phi_\beta} - V_0)}. \quad (37)$$

At spectral singularities, the wave emission probability linearly increases as a function of time t , the wave emission is a plateau characterized by Gaussian error function. High-order spectral singularities appear at $V_0 = 2i \sin k$, $V_\alpha = V_\beta = -e^{-ik}$. After scattering, the intensity increases linearly for left incidence but cubically for right incidence.

C: \mathcal{PT} -symmetric side-coupled resonators

The resonator V_0 is on resonance with other resonators on the chain ($V_0 = 0$), the side-coupled resonators $V_\alpha = -e^{-ik}$ and $V_\beta = -e^{ik}$ are \mathcal{PT} -symmetric. Substituting f_j into the equations of motion at steady state, we have

$$f_\alpha = A + B - f_0, \quad (38)$$

$$e^{ik} f_\alpha = (Ae^{-ik} + Be^{ik}) + e^{-i\phi_\alpha} f_0, \quad (39)$$

$$(e^{ik} + e^{-ik}) f_0 = (Ae^{-ik} + Be^{ik}) + (Ce^{ik} + De^{-ik}) + e^{i\phi_\alpha} f_\alpha + e^{i\phi_\beta} f_\beta, \quad (40)$$

$$e^{-ik} f_\beta = (Ce^{ik} + De^{-ik}) + e^{-i\phi_\beta} f_0, \quad (41)$$

$$f_\beta = C + D - f_0, \quad (42)$$

For left incidence ($D = 0$), we obtain

$$r_L = \frac{(e^{i\phi_\alpha} + e^{-i\phi_\alpha}) e^{-ik} - (e^{i\phi_\beta} + e^{-i\phi_\beta}) e^{ik} + (e^{-2ik} - e^{2ik})}{(e^{ik} + e^{i\phi_\alpha})(e^{-i\phi_\alpha} + e^{ik})}, t_L = -\frac{e^{-i\phi_\beta} + e^{-ik}}{e^{-i\phi_\alpha} + e^{ik}}, \quad (43)$$

For right incidence ($A = 0$), we obtain

$$r_R = 0, t_R = -\frac{e^{i\phi_\beta} + e^{-ik}}{e^{i\phi_\alpha} + e^{ik}}. \quad (44)$$

The dynamics at special cases of $|\phi_\alpha| = 2\pi/3$ and $|\phi_\beta| = 2\pi/3$ are simulated in Fig. 4. Synthetic magnetic flux at $\phi_\alpha = -2\pi/3$ ($2\pi/3$) produces a left-going (right-going) wave emission; synthetic magnetic flux at $\phi_\beta = -2\pi/3$ ($2\pi/3$) realizes a right-going (left-going) wave absorption. In Figs. 4(a) and 4(d), the system is \mathcal{PT} -symmetric. The unidirectional spectral singularities for wave emission and wave absorption coincide. The \mathcal{PT} symmetry ensures that the persistently emitted waves from resonator α are directly absorbed at resonator β and form a unity transmission. The transmission is symmetric $|t_L| = |t_R| = 1$, and the spectral singularities vanish. The snapshots presented in Figs. 4(a) and 4(d) are similar: the transmission and reflection for the left incidence are unity. However, the modal amplitudes diverge for resonator 0 when $\phi_\alpha = 2\pi/3$ and $\phi_\beta = -2\pi/3$. In addition, the difference of the magnetic fluxes results in a relative phase difference π for the transmitted waves after scattering between the left and right incidences; however, the reflections have the same phase. Figure 4(b) represents a persistent right-going wave emission for a left incidence and perfect absorption for a right incidence. Figure 4(c) illustrates a persistent left-going wave emission for right incidence and perfect reflection for left incidence. The persistent wave emissions are characterized by a Gaussian error function in Figs. 4(b) and 4(c).

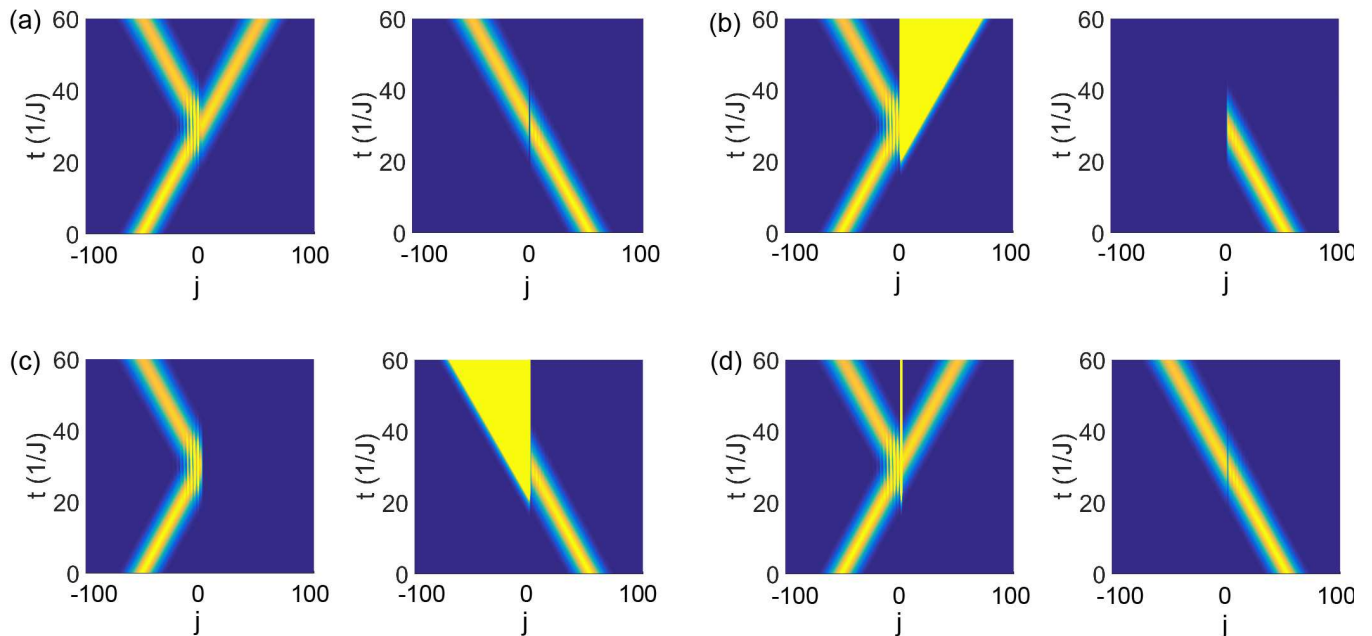


FIG. 4. Snapshots of the Gaussian wave packet dynamics for the left and right incidences at (a) $\phi_\alpha = -\phi_\beta = -2\pi/3$, (b) $\phi_\alpha = \phi_\beta = 2\pi/3$, (c) $\phi_\alpha = \phi_\beta = -2\pi/3$, and (d) $\phi_\alpha = -\phi_\beta = 2\pi/3$. They correspond to the points marked in Fig. 3(a). The system parameters are $V_\alpha = -e^{-i\pi/3}$, $V_\beta = -e^{i\pi/3}$, and $V_0 = 0$. The Gaussian wave packet with $\sigma = 0.1$ has wave vector $k_c = \pi/3$ in the simulations.

The scattering coefficients $r_{L,R}$ $t_{L,R}$ virtually share identical denominator [Eqs. (30) and (31)], but their numerators are distinct. The system is at spectral singularities when the denominator goes to zero, provided that the numerator does not vanish. When the denominator and the numerator vanish simultaneously, the coefficients are obtained by calculating the limitation of expressions as wave vector k approaches the divergent wave vector. The transmission and reflection coefficients do not diverge and the spectral singularities vanish.

D: Left lasing and right perfect absorption

The influences of the side-coupled resonators α , β vary as magnetic fluxes at different matches. The phenomenon of unidirectional lasing from one side and perfect absorbing from the other side is simulated for a Gaussian wave packet incidence in Fig. 5. The chosen synthetic magnetic fluxes are $\phi_\alpha = \phi_\beta = \pi - k$. For a left incidence, a

symmetric bidirectional lasing wave emission is created after scattering; for a right incidence, the Gaussian wave packet is perfectly absorbed without reflection.

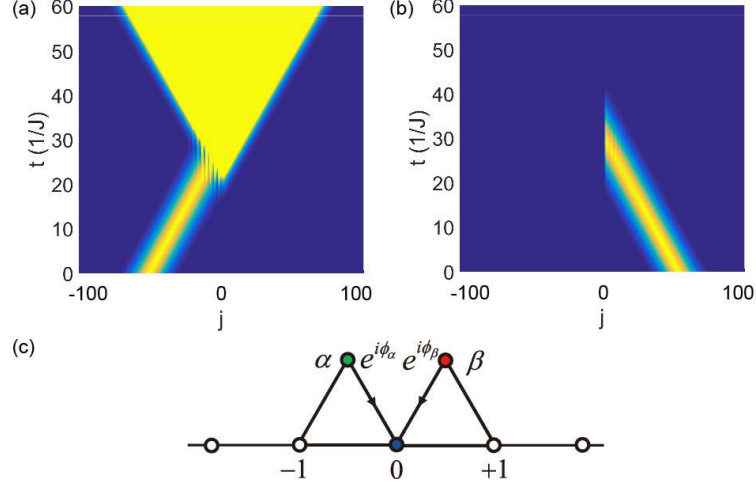


FIG. 5. Snapshots of the Gaussian wave packet dynamics for the (a) left and (b) right incidences at $\phi_\alpha = \phi_\beta = 2\pi/3$. (c) Schematic of the system with parameters $V_\alpha = -e^{-i\pi/3}$, $V_\beta = -e^{i\pi/3}$, and $V_0 = -2i \sin(\pi/3)$. The Gaussian wave packet with $\sigma = 0.1$ has wave vector $k_c = \pi/3$ in the simulations.

E: Reflectionless left unidirectional lasing and right perfect absorption

Connecting another side-coupled resonator of left full transmission and right full absorption [configuration Fig. 1(c)] on the left side of the scattering center in the situation that illustrated in Fig. 4(b), we obtain a reflectionless left unidirectional lasing and right perfect absorption. The system is schematically illustrated in Fig. 6(c). If all the synthetic magnetic fluxes in the system change into their opposite fluxes, then the dynamics will change into a left-right mirror reflection of that depicted in Figs. 6(a) and 6(b) for left and right incidences.

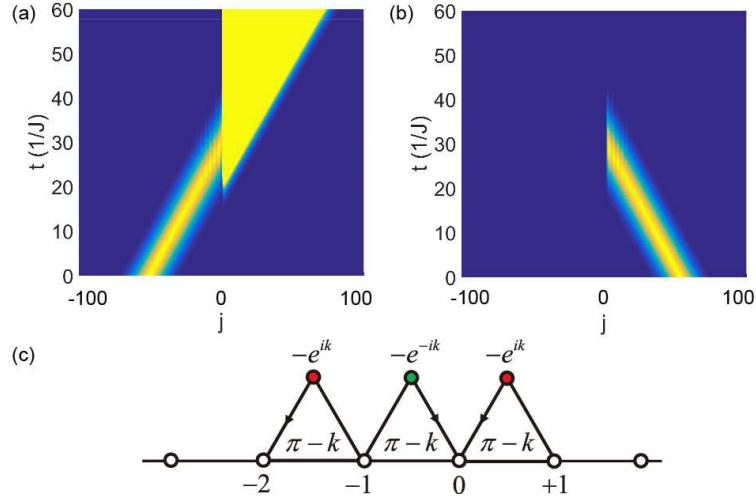


FIG. 6. Snapshots of the Gaussian wave packet dynamics for the (a) left and (b) right incidences. (c) Schematic of the system with parameters marked, $k = \pi/3$. The arrows indicate the asymmetric couplings $e^{i\phi}$ with ϕ show inside. The Gaussian wave packet with $\sigma = 0.1$ has wave vector $k_c = \pi/3$ in the simulations.

F: Transmissionless right unidirectional lasing and left perfect absorption

Connecting two left full transmission and right full absorption structures [configuration Fig. 1(c)] on the left side of the scattering center [a left-right mirror reflection of that depicted in Fig. 5(c)], we obtain a transmissionless right unidirectional lasing and left perfect absorption. The system is schematically illustrated in Fig. 7(c). If all the synthetic magnetic fluxes in the system change to their opposite fluxes, the dynamics will be unchanged.

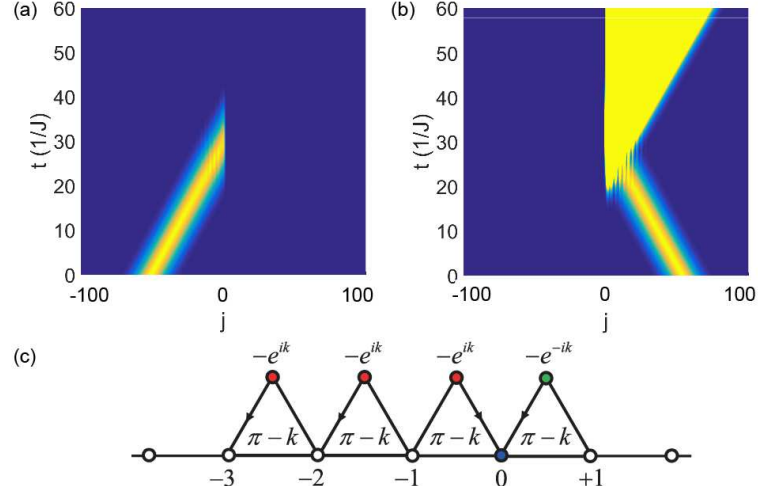


FIG. 7. Snapshots of the Gaussian wave packet dynamics for the (a) left and (b) right incidences. (c) Schematic of the system with parameters marked, $k = \pi/3$. The arrows indicate the asymmetric couplings $e^{i\phi}$ with ϕ show inside. The Gaussian wave packet with $\sigma = 0.1$ has wave vector $k_c = \pi/3$ in the simulations.